Preparation, structure and catecholase-mimetic activity of two mononuclear ferrocenecarboxylate copper(II) complexes

A. Latif Abuhijleh*,†
Department of Chemistry, Birzeit University, PO Box 14, West Bank (via Israel)
Jonathan Pollitte and Clifton Woods*
Department of Chemistry, University of Tennessee, Knoxville, TN 37996-1600 (USA)

(Received August 10, 1992; revised August 2, 1993)

Abstract

The complexes *trans*-bis(ferrocenecarboxylato)bis(pyridine)copper(II) (**2**) and *trans*-bis(ferrocenecarboxylato)-bis(imidazole)copper(II) (**3**) have been prepared from the reaction of tetrakis(ferrocenecarboxylato)bis(tetrahydrofuran)dicopper(II) (**1**) and the appropriate base. *trans*-Bis(ferrocenecarboxylato)bis(pyridine)copper(II) crystallizes as two isomers – one in which the carboxylate group coordinates in a chelating mode (**2a**) and one in which the carboxylate group coordinates as a monodentate ligand (**2b**). Complex **2a** crystallizes in the monoclinic space group $P2_1/c$ with $a=14.761(5)$, $b=5.922(2)$, $c=15.913(6)$ Å, $\beta=102.69(3)°$, $V=1357.1(8)$ Å^3, $Z=2$. The structure is compressed rhombic octahedral with four equatorial carboxylate oxygen atoms and two axial pyridine nitrogen atoms. The two Cu–O distances differ by approximately 0.2 Å suggesting that the carboxylate function bonds in an approximate chelating mode. Complexes **2b** and **3** both crystallize in the triclinic space group $P\bar{1}$ with $a=5.986(2)$, $b=8\,038(2)$, $c=15.512(3)$ Å, $\alpha=104.42(2)$, $\beta=93.11(2)$, $\gamma=99\,95(2)°$, $V=708.1(3)$ Å^3, $Z=1$, and $a=7.475(3)$, $b=9.296(3)$, $c=10.090(3)$ Å, $\alpha=111\,05(2)$, $\beta=92.38(4)$, $\gamma=101.69(3)°$, $V=635.7(4)$ Å^3, $Z=1$ for **2b** and **3**, respectively The structures of **2b** and **3** are best described as square planar with a CuN_2O_2 core having remote, weakly interacting, carboxylate oxygen atoms from the carboxylate groups at 2.53 and 2.76 Å from the copper atom for **2b** and **3**, respectively. The catalytic activities of **1**, **2** and **3** toward the aerobic oxidation of catechol to *o*-quinone were determined The activity of **2** is similar to that of **1** but much greater than that of **3** These differences are described in terms of the proposed requirement that two proximate metal atoms are involved in the catalytic process and the possible dimerization of **2** and not **3**.

Key words Crystal structures; Copper complexes; Ferrocene complexes, Carboxylate complexes

Introduction

It is well known that many dinuclear copper(II) carboxylates form dinuclear adducts with basic ligands [1]; however, with certain bases many dinuclear copper(II) carboxylates also form mononuclear adducts [1–10]. The adducts that result from the interaction of dinuclear copper(II) carboxylates with imidazole and its methyl derivatives are generally found to be mononuclear [2, 6–10], and those with pyridine are found to be binuclear [1, 5, 11–13]. Few mononuclear pyridine adducts of copper(II) complexes with non-halogenated carboxylate ligands are known [3–5]. Those complexes for which structural data are available exist as bis-adducts with the CuN_2O_2 chromophore in a *trans* square-planar arrangement [3, 4]. The mononuclear imidazole adducts of copper(II) carboxylates have been shown to exist in a variety of structures, including *cis* and *trans* bis-adducts as well as tetrakis-, pentakis- and hexakis-adducts [2, 7–10].

Because of the dependence of structure on subtle electronic and steric properties of the added bases, we investigated the structural properties of *cis*-bis(ferrocenecarboxylato)bis(1,2-dimethylimidazole)-copper(II) and *trans*-bis(ferrocenecarboxylato)bis(*N*-methylimidazole)copper(II) [8]. Cyclic voltammetric studies demonstrated that there is little electronic communication between the copper center and the ferrocenyl moieties [8]. The structural differences were assumed to be related to electronic and/or steric features associated with the location of the methyl substituents on the imidazole ligand. To examine these influences,

*Authors to whom correspondence should be addressed
†Work performed while on leave at the University of Tennessee

SSDI 0020-1693(93)03682-Z

we have used imidazole and pyridine as bases to form additional ferrocenecarboxylatocopper(II) adducts.

Since mononuclear copper(II) carboxylates with pyridines and imidazoles have been found to have a variety of pharmacological effects such as antitumor [14, 15], superoxide dismutase and catecholase activities [16, 17], structural and electronic factors that might impact these properties are of interest. In this study we examine the structures of *trans*-bis(ferrocenecarboxylato)bis(pyridine)copper(II) (**2a** and **2b**) and *trans*-bis(ferrocenecarboxylato)bis(imidazole)copper(II) (**3**), and their catalytic properties in the aerobic oxidation of catechol to *o*-quinone. These complexes might also serve as models for the copper oxidase enzyme.

Experimental

Syntheses

The compound tetrakis(ferrocenecarboxylato)bis(tetrahydrofuran)dicopper(II), $Cu_2(O_2C{-}C_5H_4{-}FeC_5H_5)_4(THF)_2 \cdot THF$ (**1**), was synthesized by the method described previously [18].

*Preparation of bis(ferrocenecarboxylato)bis(pyridine)copper(II)·1.5H$_2$O (2)**

A solution of 50 ml pyridine in 50 ml methanol was added to 0.50 g of **1**. The mixture was stirred for 1 h at 50–60 °C The dark yellow-brown solution was filtered and the filtrate was evaporated slowly under the hood. The yellow–green crystals that formed were collected and air dried. Recrystallization from hot n-butanol and pyridine (2:1) produced yellow–brown needles (**2a**) and plates (**2b**).

Anal. Found: C, 54.3; H, 4.4; N, 3.7. Calc. for $C_{32}H_{38}CuFe_2N_2O_4 \cdot 1.5H_2O$ (**2**): C, 54.4; H, 4.4; N, 3.9%.

Preparation of bis(ferrocenecarboxylato)bis(imidazole)copper(II) (3)

A solution of 0.14 g (2.06 mmol) of imidazole in 50 ml of methanol was added to 0.54 g (0.43 mmol) of **1**. The mixture was stirred for 2 h in an ice bath. The yellowish brown precipitate that formed was filtered, washed with cold methanol, and air dried. A second crop was obtained from the yellow–brown filtrate. When the filtrate was layered with anhydrous diethyl ether concentrated by slow evaporation under the hood to *c.* 10 ml, an amorphous product appeared which was removed by filtration. The resulting solution was evaporated slowly to produce yellow–brown crystals.

Anal. Found: C, 50.9; H, 4.0; N, 8.4 Calc. for $C_{28}H_{26}CuFe_2N_4O_4$ (**3**): C, 51.1; H, 4.0; N, 8.5%.

Physical measurements

Room temperature (298 K) magnetic susceptibility, diffuse reflectance UV–Vis, IR and EPR spectral measurements of solid samples were obtained as described previously [8]. Elemental analyses for C, H and N were performed by Galbraith Laboratories, Knoxville, TN, USA.

Catecholase-mimetic activities

Because of the low solubility of **2** and **3** in most organic solvents, the oxidation of catechol was performed by adding the solids to methanol solutions of catechol. In a typical experiment 10 mg of the compound was added to 100 ml of a methanol solution (0.1 M) of catechol. The mixture was stirred and the compound dissolved within 1–2 min. Aliquots of the mixture were taken at 4 min intervals, and placed in 1 cm quartz cells. The *o*-quinone absorbance at 390 nm was monitored spectrophotometrically as a function of time at 25 °C on a Hewlett Packard 8452A diode array spectrophotometer.

Crystal structure determinations

Crystallographic data for **2a**, **2b** and **3** are listed in Table 1. Intensity measurements were made on a Siemens R3m/V diffractometer at 163 K for **2a** and **3** and at 293 K for **2b**. Refined unit-cell parameters for **2a**, **2b** and **3** were derived by least-squares treatment of a group of high diffractometer setting angles. The intensities of three standard reflections were monitored every 97 reflections and no significant variations in intensities were observed during the data collection for any complex. The intensity data were corrected for Lorentz and polarization effects The absorption coefficients were 18.8, 18.0 and 20.0 cm^{-1} for **2a**, **2b** and **3**, respectively. An empirical absorption correction based on the method of Hope was applied to the intensity data [19].

The crystal structure was solved by heavy atom (Patterson and difference Fourier) methods [20]. Full-matrix least-squares adjustment of positional and anisotropic thermal parameters, with hydrogen atoms included at their calculated positions during final iterations, converged to the residuals listed in Table 1 Table 1 also contains a summary of the crystallographic data. See also 'Supplementary material'.

Results and discussion

Magnetic and spectroscopic results

The solid-state magnetic and spectroscopic data for complexes **2** and **3** are summarized in Table 2. The

*Compound **2** crystallizes in two different morphologies, **2a** and **2b**. It is likely that there is one structure of interconversion between **2a** and **2b**

TABLE 1. Crystal data for *trans*-[Cu($O_2CC_5H_4FeC_5H_5)_2$(py)$_2$] (**2a, b**) and *trans*-[Cu($O_2CC_5H_4FeC_5H_5)_2$(imid)$_2$] (**3**)[a]

Molecular formula	$C_{32}H_{38}CuFe_2N_2O_4$ (**2a**)	$C_{32}H_{38}CuFe_2N_2O_4$ (**2b**)	$C_{28}H_{26}CuFe_2N_4O_4$ (**3**)
Formula weight	679.8	679.8	657.8
Space group	$P2_1/c$	$P\bar{1}$	$P\bar{1}$
Z	2	1	1
a (Å)	14.761(5)	5.986(2)	7 475(3)
b (Å)	5 922(2)	8 038(2)	9 296(3)
c (Å)	15.913(6)	15 512(3)	10.090(3)
α (°)	90	104.42(2)	111 05(2)
β (°)	102.69(3)	93 11(2)	92 38(4)
γ (°)	90	99 95(2)	101 69(3)
V (Å^3)	1357 1(8)	708.2(3)	635.7(4)
D_{calc} (g/cm^3)	1 502	1 594	1 496
Crystal size (mm)	0 25×0 65×0.70	0 50×0.40×0.20	0 15×0.22×0 60
Radiation type; wavelength (Å)		Mo; 0 71073	
Temperature (K)	163	293	163
Absorption coefficient (cm^{-1})	18 6	18 0	17 2
R (%)	4 67	4 50	8 32
R_w (%)	4 21	5 32	10.84
Goodness-of-fit	1 47	1 69	1 26

[a]py = pyridine, imid = imidazole

TABLE 2 Magnetic moments, ESR, electronic and IR data for complexes **2** and **3**[a,b]

Complex	μ_{eff} (BM)	$g_\perp$	$g_\parallel$	λ_{max} (nm)	$\nu_{asym}(CO_2)$ (cm^{-1})	$\nu_{sym}(CO_2)$ (cm^{-1})
2	1.83	2.05	2.18	660,458	1575	1380
3	1 87	2.06	2 23	670,455	1560[c]	1394

[a]These data are for polycrystalline samples at room temperature [b]**2** is taken to be a polycrystalline mixture of **2a** and **2b**. [c]Broad band overlaps with the imidazole absorption band

room temperature (298 K) magnetic moment in each case is consistent with the presence of one unpaired electron in a monomeric copper(II) complex. The UV–Vis diffuse reflectance spectra of the two complexes exhibit broad low-energy electronic bands centered at about 660 and 670 nm for **2** and **3**, respectively. A more intense band occurs near 455 nm (Table 2). The lower energy band is assigned to the copper(II) d–d transitions. The position of the band is consistent with the assignments for other tetragonally distorted copper(II) complexes containing a CuN_2O_4 or $CuN_2O_2\cdots O_2$ chromophore [1b, 7, 8, 21]. It is comparable to those found for mononuclear ferrocenecarboxylate copper(II) complexes with the *N*-methyl and 1,2-dimethyl imidazole derivatives [8]. The higher energy band is the characteristic band of the ferrocenyl moiety which occurs at 460 nm for the free acid. The small shift in its position upon complexation suggests that there is very little perturbation of the molecular orbitals of the ferrocenyl moiety by the copper(II) ion and the other ancillary ligands This conclusion is consistent with the previous electronic and cyclic voltammetric studies obtained for the adducts with methylimidazoles [8].

The IR absorptions for the ferrocenecarboxyl antisymmetric, $\nu_{asym}(CO_2)$, and symmetric, $\nu_{sym}(CO_2)$, stretching frequencies are compared in Table 2. The $\nu_{sym}(CO_2)$ for **3** is not resolved, but overlaps with the imidazole band to give an intense and broad absorption band centered at 1560 cm^{-1}. The positions of $\nu_{asym}(CO_2)$ and $\nu_{sym}(CO_2)$ and their separation, $\Delta\nu$, for **2** and **3** are comparable to those reported for mononuclear ferrocenecarboxylate copper(II) complexes with methylimidazoles whose structure determinations show that the carboxylate ligand coordinates in an 'unsymmetrical' bidentate mode [8].

X-band EPR spectral parameters of polycrystalline samples of **2** and **3** are given in Table 2. These data are characteristic of elongated tetragonal mononuclear copper(II) complexes [21]. The EPR spectrum for the two complexes are anisotropic with $g_\parallel$ and $g_\perp$ components. The lack of copper(II) hyperfine coupling is likely due to dipolar interactions between copper atoms of neighboring molecules. These spectral data are consistent with the presence of the CuN_2O_4 or $CuN_2O_2\cdots O_2$ chromophore [7, 8, 21].

*Structures of trans-(O_2C–C_5H_4–$FeC_5H_5)_2$(py)$_2$Cu (**2a, b**) and trans-(O_2C–C_5H_4–$FeC_5H_5)_2$(imid)$_2$Cu (**3**)*

Atomic coordinates for **2a**, **2b** and **3** are given in Tables 3, 4 and 5, respectively. Selected bond lengths and bond angles are given in Table 6. The structures for **2a**, **2b** and **3** are shown in Figs. 1, 2 and 3, respectively. Complex **2a** exists as a compressed rhombic octahedral with a six-coordinate copper atom in a plane of four donor oxygen atoms from two ferrocenecarboxylate

TABLE 3. Atomic coordinates ($\times 10^4$) and equivalent isotropic displacement coefficients ($Å^2 \times 10^3$) for **2a**

	x	y	z	U_{eq}[a]
Cu	0	5000	0	31(1)
Fe	3581(1)	2235(1)	614(1)	15(1)
O(1)	1299(3)	5140(8)	−365(3)	34(2)
O(2)	921(3)	1830(9)	85(3)	36(2)
C(1)	1482(4)	3074(13)	−175(4)	25(2)
C(2)	2375(4)	2165(11)	−298(3)	15(2)
C(3)	3074(4)	3353(10)	−610(3)	18(2)
C(4)	3826(4)	1891(12)	−603(4)	25(2)
C(5)	3605(4)	−225(12)	−281(4)	25(2)
C(6)	2700(4)	−68(11)	−95(3)	19(2)
C(7)	3670(5)	1529(12)	1886(4)	32(3)
C(8)	3286(5)	3696(12)	1683(4)	29(3)
C(9)	3936(5)	4995(12)	1375(4)	30(2)
C(10)	4739(4)	3615(12)	1390(4)	28(3)
C(11)	4562(4)	1500(12)	1706(4)	24(2)
N(1)	619(3)	5736(10)	1201(3)	22(2)
C(12)	1031(4)	7721(13)	1418(4)	32(3)
C(13)	1450(5)	8246(13)	2264(5)	38(3)
C(14)	1447(5)	6701(13)	2900(4)	32(3)
C(15)	1025(4)	4663(13)	2681(4)	32(3)
C(16)	620(4)	4218(12)	1825(4)	26(2)

[a]Equivalent isotropic U defined as one third of the trace of the orthogonalized U_{ij} tensor.

TABLE 4 Atomic coordinates ($\times 10^4$) and equivalent isotropic displacement coefficients ($Å^2 \times 10^3$) for **2b**

	x	y	z	U_{eq}[a]
Cu	0	0	0	41(1)
Fe	2204(1)	2441(1)	3576(1)	47(1)
N(1)	1988(8)	1565(6)	−585(3)	43(2)
O(1)	2091(6)	942(5)	1111(2)	45(1)
O(2)	−565(7)	2555(5)	1248(3)	53(2)
C(1)	1217(10)	2192(7)	1546(3)	42(2)
C(2)	2385(10)	3211(7)	2423(3)	41(2)
C(3)	4606(10)	3128(8)	2777(4)	49(2)
C(4)	5058(12)	4302(8)	3645(4)	58(3)
C(5)	3149(12)	5110(8)	3821(4)	60(3)
C(6)	1503(11)	4441(7)	3069(4)	51(2)
C(7)	245(14)	4(9)	3271(5)	73(3)
C(8)	2384(14)	−9(9)	3678(5)	71(3)
C(9)	2688(13)	1145(9)	4531(5)	67(3)
C(10)	761(14)	1871(9)	4648(5)	70(3)
C(11)	−772(12)	1156(10)	3875(6)	75(3)
C(12)	1522(11)	3067(7)	−683(4)	56(3)
C(13)	2827(13)	4096(8)	−1127(5)	74(3)
C(14)	4696(14)	3562(10)	−1474(5)	80(4)
C(15)	5216(11)	2030(8)	−1383(4)	64(3)
C(16)	3847(10)	1056(7)	−932(4)	47(2)

[a]Equivalent isotropic U defined as one third of the trace of the orthogonalized U_{ij} tensor

ligands The two remaining donor atoms are the pyridine nitrogen atoms in a *trans* disposition above and below the plane of oxygen atoms. The copper atoms lie on an inversion center at 0, 1/2, 0. The two Cu–O distances

TABLE 5 Atomic coordinates ($\times 10^4$) and equivalent isotropic displacement coefficients ($Å^2 \times 10^3$) for **3**

	x	y	z	U_{eq}[a]
Cu	0	0	0	73(1)
Fe	−1831(2)	3383(2)	−3302(2)	75(1)
N(1)	1948(12)	−936(10)	−947(9)	71(4)
N(2)	4539(13)	−1130(11)	−1878(10)	82(4)
C(1)	3371(15)	−194(13)	−1402(12)	77(5)
C(2)	3907(16)	−2515(14)	−1694(12)	84(5)
C(3)	2315(15)	−2386(13)	−1121(11)	77(5)
O(1)	384(10)	1464(8)	−1008(8)	79(3)
O(2)	−1943(10)	−375(8)	−2534(8)	79(3)
C(4)	−705(16)	906(13)	−2177(11)	73(5)
C(5)	−444(14)	1771(12)	−3151(12)	77(5)
C(6)	−1349(15)	1292(13)	−4543(11)	79(5)
C(7)	−647(16)	2445(13)	−5076(13)	81(5)
C(8)	679(16)	3665(14)	−4070(12)	80(5)
C(9)	807(15)	3276(13)	−2852(13)	78(5)
C(10)	−2703(18)	5422(15)	−2907(13)	88(6)
C(11)	−3960(19)	4106(17)	−3915(15)	100(7)
C(12)	−4616(19)	3026(15)	−3278(15)	94(6)
C(13)	−3752(16)	3600(13)	−1913(13)	81(5)
C(14)	−2539(15)	5109(13)	−1642(12)	81(5)

[a]Equivalent isotropic U defined as one third of the trace of the orthogonalized U_{ij} tensor.

are 2.123(5) and 2.304(5) Å for Cu–O(1) and Cu–O(2), respectively. These distances indicate that the carboxylate function acts more like a chelating group than a monodentate carboxylate function with very weak interaction of the second oxygen atom. The Cu–N(1) distance is 1.977(5) Å. The O(1)–C(1)–O(2) angle is 121.7(6)°, and the C(1)–O(1)–Cu and C(1)–O(2)–Cu angles are 93.2(4) and 85.7(4)°, respectively, for **2a**. At 293 K, $\Delta O = 0.12$ Å (versus $\Delta O = 0.18$ at 163 K) with Cu–O(1) and Cu–O(2) distances of 2.165(7) and 2.282(8), respectively. However, the estimated standard deviations render the differences in the Cu–N(1) and Cu–O(2) bond lengths at 163 and 293 K insignificant at the 3σ level. Therefore, the structures at high and low temperatures are not consistent with significant solid state fluxionality.

The structure of **2b** is best described as square planar with weak off-the-z-axis bonding with the $CuN_2O_2 \cdot\cdot O_2$ chromophore. The remote oxygen atoms of the carboxylate ligands are 2.53 Å away from the copper atoms and are best described as weakly interacting. The Cu–O distance for the strongly interacting oxygens is 1.975(3) Å, approximately 0.15 Å shorter than the shortest Cu–O bond distance in **2a**. The O(1)–C(1)–O(2) angle is 122.1(4)° The C(1)–O(1)–Cu angle is 102.9(3)°, 9.7° larger than that for the corresponding angle in **2a**, while the C(1)–O(2)–Cu angle is 77.9°, 7.8° smaller than in **2a**.

The structure of **3** resembles that of **2b**. It is best described as four-coordinate square planar with weak

TABLE 6 Selected bond lengths (Å) and bond angles (°) for **2a**, **2b** and **3**

Bond lengths					
2a					
Cu–O(1)	2.123(5)	Cu–O(2)	2 304(5)	Cu–N(1)	1 977(5)
O(1)–C(1)	1.275(9)	O(2)–C(1)	1 245(9)	C(1)–C(2)	1.476(9)
2b					
Cu–O(1)	1.975(3)	Cu–N(1)	1 998(5)	O(1)–C(1)	1 273(7)
O(2)–C(1)	1.248(8)	C(1)–C(2)	1 468(7)		
3					
Cu–N(1)	1.955(9)	Cu–O(1)	1 957(9)	O(1)–C(4)	1 278(13)
O(2)–C(4)	1.273(12)	C(4)–C(5)	1 473(19)		
Bond angles					
2a					
O(1)–Cu–O(2)	59.4(2)	O(1)–Cu–N(1)	90 1(2)		
O(2)–Cu–N(1)	88.9(2)	Cu–O(1)–C(1)	93 2(4)		
Cu–O(2)–C(1)	85.7(4)	O(1)–C(1)–O(2)	121 7(6)		
O(1)–C(1)–C(2)	117 9(6)	O(2)–C(1)–C(2)	120 4(6)		
2b					
O(1)–Cu–N(1)	89.5(2)	Cu–O(1)–C(1)	102 9(3)		
O(1)–C(1)–O(2)	122.1(4)	O(1)–C(1)–C(2)	117 5(5)		
O(2)–C(1)–C(2)	120 4(5)				
3					
N(1)–Cu–O(1)	88.8(4)	Cu–O(1)–C(4)	110 6(7)		
O(1)–C(4)–O(2)	122 5(12)	O(2)–C(4)–C(5)	120 0(9)		
O(1)–C(4)–C(5)	117 5(9)				

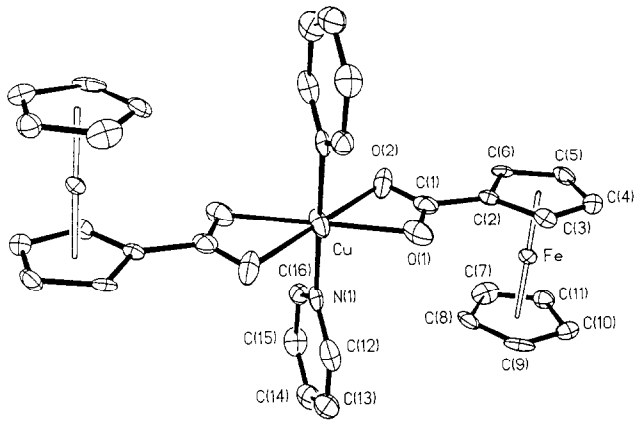

Fig 1. Structure of *trans*-[Cu($O_2CC_5H_4FeC_5H_5$)$_2$(py)$_2$] (**2a**) with hydrogen atoms omitted for clarity.

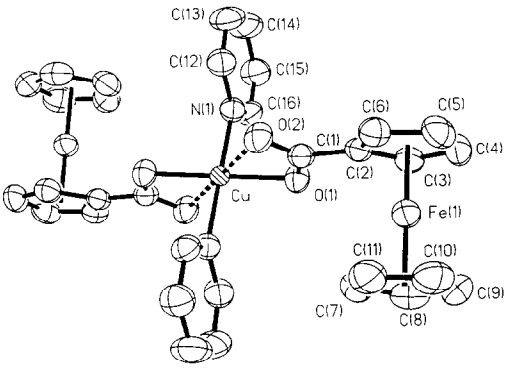

Fig 2. Structure of *trans*-[Cu($O_2CC_5H_4FeC_5H_5$)$_2$(py)$_2$] (**2b**) with hydrogen atoms omitted for clarity

off-the-*z*-axis bonding with the $CuN_2O_2\cdots O_2$ chromophore. The more remote oxygen atoms of the carboxylate ligands are more accurately described as weakly interacting since the Cu–O distance for the oxygen atoms is 2.76 Å. This is 0.23 Å longer than the corresponding bonds in **2b**, indicating even weaker off-the-*z*-axis bonding than seen in **2b**. The Cu–O distance for the copper-bound carboxylate oxygen atoms is 1.957(9) Å, approximately 0.16 and 0.02 Å shorter than the shortest Cu–O distances in **2a** and **2b**, respectively. The Cu–O(1)–C(4) angle is 110.6(7)°, much greater than the Cu–O–C angles in **2a** but only 7.7° greater

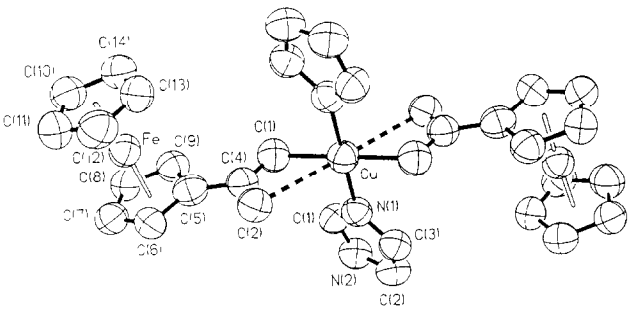

Fig. 3 Structure of *trans*-[Cu($O_2CC_5H_4FeC_5H_5$)$_2$(imid)$_2$] (**3**) with hydrogen atoms omitted for clarity

than that for **2b**. These differences between **2a, 2b** and **3** are consistent with the approximate chelating mode of the carboxylate ligands in **2a** and the approximate monodentate binding mode of the carboxylate ligands in **2b** and **3**. The Cu–N distance in **3** is 1.955(9) Å.

All Fe–C distances for **2a, 2b** and **3** are comparable to those observed for other complexes that contain the ferrocenecarboxylate ligands [8, 18]. The C_5H_4 and C_5H_5 rings are essentially eclipsed in all three of the above complexes, although they have been observed to be staggered in other complexes [18].

Catecholase-mimetic activity

The rates of the catalyzed oxidation of catechol to *o*-quinone by **2** and **3** were determined and compared to that of **1**. The oxidation was monitored by recording the change in absorbance of *o*-quinone at 390 nm with time for the first 30 min of the reaction. These results are shown in Fig. 4. The enzyme-mimetic activities of the copper complexes were determined as micromoles of *o*-quinone produced per mg of catalyst per min. These values are 0.20, 0.17 and 0.07 for **1, 2** and **3**, respectively. Although *o*-quinone is produced in the presence of these complexes, the rate at which it is produced varies significantly with the nature of the catalyst. The relatively high catalytic activity of **1** (Fig. 4) may be associated with a binuclear entity such as that found in the copper-containing enzyme tyrosinase and binuclear copper(II) synthetic models. In these instances it is believed that during the oxidation of catechol to *o*-quinone the two proximate metal atoms bond to the two hydroxyl oxygen atoms of the catechol [22–24]. Although mononuclear copper(II) complexes exhibit catecholase-mimetic activities, these are usually lower than those of dinuclear copper complexes [22b, 23]. For non-planar mononuclear copper(II) complexes, it has been proposed that the two copper(II) atoms must be located at a distance of less than 5 Å for bonding to the catechol hydroxyl groups, a mode which should facilitate electron transfer to dioxygen [23]. The explanation for the higher catalytic activity of the mononuclear bis-pyridine adduct **2** compared to the bis-imidazole adduct **3** is not immediately obvious but dimerization of the complex in solution to provide two proximate metal sites cannot be ruled out since dimerization is known for other bis-pyridine adducts of copper(II) carboxylates [25] Dimerization of bis-imidazole adducts of copper(II) carboxylates is not known and the only known binuclear complex of copper(II) carboxylates with imidazoles is the benzimidazole monoadduct of copper(II) acetate [26]. This could explain the lower catecholase-mimetic activity of the bis-imidazole complex.

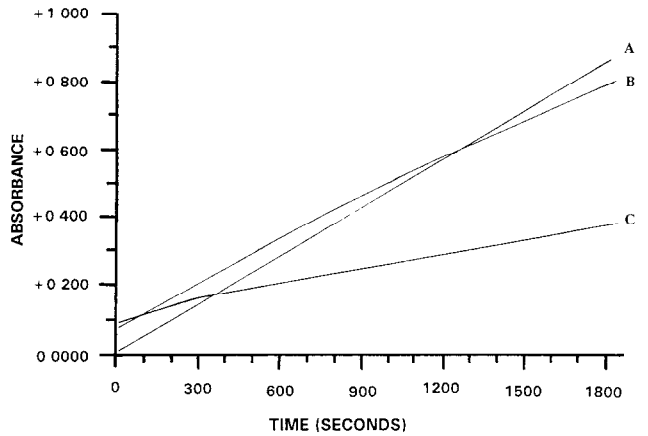

Fig. 4. Plot of absorbance vs. time for the oxidation of catechol catalyzed by **1** (A), **2** (B) and **3** (C).

Supplementary material

Complete tables of bond lengths and angles, anisotropic thermal parameters, and observed and calculated structure factors are available from the authors on request.

Acknowledgements

The authors thank Research Corporation for partial support. A.L.A. acknowledges the partial support of this work by Birzeit University under Grant No. 86/68/97.

References

1 (a) R J. Doedens, *Prog Inorg Chem, 21* (1976) 209, (b) N. Melnik, *Coord Chem Rev, 36* (1981) 1, (c) M. Kato and Y. Muto, *Coord Chem Rev., 92* (1988) 45
2 H.A. Henriksson, *Acta Crystallogr, Sect B, 33* (1977) 1947.
3 N E. Heimer and I Y. Ahmed, *Inorg Chim Acta, 64* (1982) L65
4 F T Greenaway, A. Pezesh, A.W Cordes, M.C Nobel and J R J. Sorenson, *Inorg Chim Acta, 93* (1984) 67
5 I Y Ahmed and A.L. Abuhijleh, *Inorg Chim Acta, 61* (1982) 241
6 A Latif Abuhijleh, *Polyhedron, 8* (1989) 2777.
7 A.L Abuhijleh, C Woods and I Y. Ahmed, *Inorg Chim Acta, 190* (1991) 11.
8 A L Abuhijleh and C. Woods, *J Chem Soc, Dalton Trans*, (1992) 1249.
9 A L Abuhijleh and C. Woods, *Inorg Chim Acta, 194* (1992) 9.
10 A L Abuhijleh and C. Woods, unpublished results
11 E Kokot and R L Martin, *Inorg Chem., 3* (1964) 1306
12 F. Hanic, D. Stenpelova and K Hanicova, *Acta Crystallogr, 17* (1964) 633
13 M V Hanson, C B. Smith, W.E. Marsh and G O Carlisle, *J Mol Struct, 37* (1977) 329.

14 J.R.J Sorenson, *Prog Med Chem*, *26* (1989) 437, and refs. therein
15 H. Tamura, H. Imai, J. Kuwahara and Y. Sugiura, *J Am Chem Soc*, *109* (1987) 6870
16 R.G. Bhirud and T S. Srivastava, *Inorg Chim. Acta, 173* (1990) 121.
17 A.L. Abuhijleh, C Woods, E. Bogas and G. LeGuenniou, *Inorg Chim Acta, 195* (1992) 67.
18 M.R. Churchill, Y.J. Li, D Nalewajek, P.M. Schaber and J. Dorfman, *Inorg Chem*, *24* (1985) 2684.
19 H. Hope and J G. Moezzi, Department of Chemistry, University of California, Davis, CA, 1988, personal communication
20 G.M. Sheldrick, *SHELXTL PLUS Structure Solution Package,* Version 4.1, Siemens Analytical X-ray Instruments, Inc., Madison, WI, USA, 1990
21 B.J. Hathaway and D E Billing, *Coord Chem Rev*, *5* (1970) 143.
22 (a) M A. Cabras and M.A. Zoroddu, *Inorg Chim Acta, 135* (1987) L19, (b) M.R. Malachowski and M G Davidson, *Inorg Chim Acta, 162* (1989) 199.
23 K.D Karlin and Y. Gultneh, *Prog Inorg Chem*, *35* (1987) 219, and refs. therein
24 D.E. Wilcox, A G Porras, Y.T. Hwang, K. Lerch, M.E. Winkler and E.I. Solomon, *J Am Chem. Soc.*, *107* (1985) 4015
25 (a) A L. Abuhijleh and I Y Ahmed, *Polyhedron, 10* (1991) 793; (b) I Urska, *J Chem Soc, Dalton Trans*, (1991) 2747, and refs. therein
26 M. Bukowska-Strzyzewska, J Showeranda and A. Tosik, *Acta Crystallogr, Sect B, 38* (1982) 2904